

## Characteristics of pressure drop during the pulse-jet cleaning of a ceramic filter for high temperature and high pressure

Jin-Hyoung Kim, Young-Chul Kim, and Joo-Hong Choi<sup>†</sup>

Department of Chemical Engineering/ERI, Gyeongsang National University, 501, Jinju-daero, Jinju 52828, Korea  
(Received 14 March 2015 • accepted 11 October 2015)

**Abstract**—The operation range of the pressure drop between the peak and the base line during the pulse-jet cleaning of a ceramic filter relates closely with the grouping number of the filter elements in the filter unit, as well as the design and the operation conditions of the pulse cleaning system. A semi-empirical model was developed to predict the pressure drop of the filter unit versus the operation time according to the grouping numbers of the total filter elements in this study. The model is based on theoretical considerations and the application of the experimental data to develop a simple equation, which should be useful for preliminary design and operational inspection. The semi-empirical formula predicts the operational values of the pressure drop between the peak and the base line, which suggests the guideline for grouping of the filter elements for the pulse-jet cleaning. Peak pressure drop decreases gradually and then finally approaches a minimum stable value as the number of the cleaning group increases. Otherwise, the base line pressure drop increases gradually and then finally approaches a maximum stable value as the number of the cleaning group increases. Thus, the gaps between the peak and the base line pressure drop become narrow as the number of cleaning group increases. This phenomenon of gap reduction is desirable for the pulse cleaning of the filter element as it reduces the pulse cleaning load. Moreover, pulse cleaning becomes more effective as the number of the cleaning groups increases.

Keywords: Pulse-jet, Pressure Drop, Ceramic Filter, Group Filter, Semi-empirical Model, Dust Collection

### INTRODUCTION

Ceramic filter elements have been known as advanced materials for particulate removal filter units at high temperature and high pressure, especially for combined cycle power systems such as integration gasification combined cycle (IGCC) and pressurized fluidized bed combustion (PFBC). The advantages of the ceramic barrier filters come from their high capability for superior particulate collection efficiency with a relatively low pressure drop [1-3], as well as their wide adaptability in the variant size and the severe operational conditions. The most common shape of the ceramic filter element is the candle type, which is a hollow cylinder closed at one end and opened at its mouth. The outside diameter and length of the typical filter element is 0.06 and 1.5 m (ranging from 1 to 3 m depending on the material [2]), respectively. A large number of filter element are necessary for the commercial filter unit. It is reported [1] that the number of candles for a 300 MWe plant is 800, 1,500, and 9,600 elements for IGCC (oxygen blown), IGCC (air blown), and PFBC, respectively. Thus, it is important to arrange such a huge number of filter elements in the filter vessel. The grouping of the filter elements as a proper number is one of the key technologies for the filter unit design. Schumacher arranged 864 filter candles in 18 groups, where 48 elements were arrayed for every group for a 250 MWe IGCC plant at Buggenum in the Nether-

lands [4]. Schumacher's unit consists of a single tube sheet where the filter elements are mounted on a single venturi for every cluster so filter elements are cleaned cluster by cluster through the venturi ejector, which provides a uniform pressure distribution on every filter element in a cluster.

Periodical pulse cleaning of filter elements is the typical method for maintaining a constant pressure loss of the filter unit. A strong pulse-jet of high-pressure gas is injected into the mouth of the filter elements in the pulse-jet method for filter cleaning. Filter cleaning is based on the fixed time interval or on the pressure of which a pre-set peak pressure drop is reached. One part among the total filter elements is exposed to the momentum of the pulse-jet at the time of pulse cleaning. The choice about how many fractions of the total filter elements is subjected to the cleaning depends on the grouping strategy of the filter elements. One group among total (n) groups is cleaned sequentially at the end of a filtering cycle while others are carrying out the filtration. A fraction of dust cake attached on the filter surface is dislodged with the pulse impaction and settles down in the filter unit. Thus, the cleaning mechanism, in case of the rigid filter element, depends mainly on the momentum originating from the reverse flow of the pulse gas, which involves the secondary gas formed during the pulse gas injection.

The efficiency of filter cleaning depends on many factors, such as cleaning method, design technologies of the cleaning system, properties of the particulate and gas, operational condition, operational method, and so on. Many workers are studying the filtration mechanism and optimization of the pulse system for a single filter element [5-13], but there are few studies [14] on the group filter

<sup>†</sup>To whom correspondence should be addressed.

E-mail: jhchoi@gnu.ac.kr

Copyright by The Korean Institute of Chemical Engineers.

system. The cleaning efficiency of the filter element in the group filter system may be governed with several factors originating in the interaction between one filter and another filter, as well as one group and another group. Thus, the intensity of pulse momentum developed in the ongoing filter element is subjected to cleaning, as well as to the walking of the detached dust cake. Some parts of the dust cake dislodged from the filter surface may be re-deposited on the filter surface if they are entrained with the strong force of gas flow on the right direction of filtration mode, thus becoming the reason for the bad cleaning efficiency of the filter element. The environment of a strong interaction between one group and another group of filter elements may be formed when the grouping number is so little or so large. Moreover, the number of the filter element group has a considerable relation with the excessive pressure difference across the tube-sheet, causing elemental lifting, which is one of the main reasons for the failure of the filter unit [3]. Thus, the grouping of the filter element for pulse jet is a primary task in designing an effective filter unit.

The efficiency of filter cleaning is commonly monitored with the observation of the pressure drop change after the end of the pulse cleaning of every group. When the cleaning efficiency is perfect, the pressure drop returns the original minimum value of the state where the pulse cleaning starts for every cycle. However, a slight increase of the base line pressure drop involves during the long-term operation of the filter unit even though this is not readily detected in the short term operation during the normal operation condition. The estimation of the pressure drop change according to the variation of group number is the goal of this study. It is assumed that the complete surface of the all filter elements subjected to the pulse jet is cleaned uniformly. The experimental observations of pressure drops are also carried out to validate the semi-empirical formula.

### THEORETICAL BACKGROUND

Fig. 1(a) shows a typical pattern of the pressure drops observed in an experimental filter unit during the initial stage of the filtration time using the fresh filter elements [15]. The overall pressure drop of the filter unit ( $\Delta P_T$ ) indicates the pressure difference between

the inside and the outside of the filter element, and presents the sum of the pressure drops across the filter element only ( $\Delta P_F$ ), the residual dust cake ( $\Delta P_R$ ), and the temporary dust cake ( $\Delta P_C$ ) as denoted in Eq. (1). Those three components of pressure drop can be isolated individually in an experiment by subtracting each from each using the preliminary measurement of  $\Delta P_F$  for the fresh filter element under the ash-free condition. The pressure drops contributed from each source are described schematically in Fig. 1(b). At a certain time, one cycle of filtration starts right after a pulse cleaning carried out and particles start to be accumulated on the filter elements again. Thus, pressure drop increases from  $\Delta P_i$  and reaches a certain pressure drop ( $\Delta P$ ) during the run time ( $t_{i+1} - t_i$ ), where  $\Delta P$  is the peak pressure drop at the moment of the successive pulse cleaning.  $\Delta P_{i+1}$  is the pressure drop at the right time after the pulse cleaning is carried out, which is the base line pressure drop. The locus of  $\Delta P_i$  constructs the base line pressure drop ( $\Delta P_B$ ), which is the sum of  $\Delta P_F$  and  $\Delta P_R$ . The base line pressure drop is recovered on the level of  $\Delta P_{i+1}$  right after the pulse cleaning.  $\Delta P_C$  and  $\Delta P_R$  represent  $(\Delta P - \Delta P_i)$  and  $(\Delta P_{i+1} - \Delta P_i)$ , respectively.

$$\Delta P_T = \Delta P_F + \Delta P_R + \Delta P_C = \Delta P_B + \Delta P_C \quad (1)$$

The increase of  $\Delta P_R$  is mainly due to the remaining dust cakes which are not removed during the pulse cleaning process. It is difficult to predict this value with a simple equation. It co-dependes with many factors such as the property of the residual dust cake remaining on the filter surface, pressure resistance through the pores which are plugged with the particles penetrating, and the pore size reduction of dust cake due to compression under the high drag force of the flow gas. We obtained this value by an experimental study. In experimental observation, the increasing rate of  $\Delta P_R$  is generally low in the normal operation condition of the filter unit and can be expressed as a linear dependency on the run time like Eq. (2) by ignoring the rapid rising at the initial operation term. The rising rate of the residual pressure drop ( $r_R$ ) is defined by Eq. (3) and is nearly zero for the perfect cleaning of the filter element in order to sustain it for several years. In practice, it lies under the range of around  $1.0 \times 10^{-3}$  Pa/h in the experimental observations [16-18].

$$\Delta P_R = r_R t \quad (2)$$

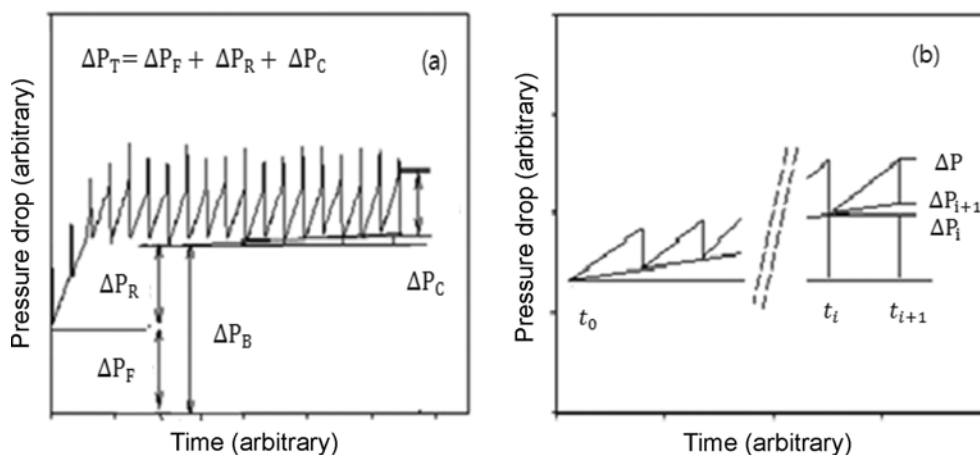


Fig. 1. Expression of the pressure drops in a filter unit during the pulse cleaning of the filter element.

$$r_R = \frac{(\Delta P_{i+1} - \Delta P_i)}{(t_{i+1} - t_i)} \tag{3}$$

The pressure drop across the temporary dust cake ( $\Delta P_C$ ) is also governed by many co-dependent factors originating from the properties of particulate, gas, and the operation conditions, as well as the pulse cleaning system. Moreover, the compression property of the dust cake makes the task more difficult in terms of predicting the value exactly with a simple equation [19,20]. The compression phenomenon of the dust cake is also governed by several effects such as the particle properties (shape, size, and density) [16-18], the gas properties (density, viscosity, and humidity) [21], the operation conditions (the face velocity and the cleaning method) [22,23], and the operation temperature [24]. In general, the pattern of  $\Delta P_C$  shows an upward curvature according to the mass load [18], which means the increasing rate of  $\Delta P_C$  is low in the early stage of the dust layer formation, but considerably increases as its thickness grows for long-time filtration. This phenomenon indicates that the compression of the dust cake appeared after its considerable thickness formed with a multilayer structure of the dust cake.

Though it is too complicated to express  $\Delta P_C$ , a simple approach of linear increase in pressure drop versus time is approximately acceptable [24], especially for the case of the non-compressible particulate or at the operation condition in low face velocity [25]. The linear assumption of  $\Delta P_C$  is also reasonable in case of a relatively thin layer of dust cake formed during the short-time filtration in which the short duration of pulse cleaning cycle is kept. In this study, the simple and linear approach about the pressure drop rising across the individual filter element is emphasized as the total pressure drop of the filter unit is more dominant with the number of the filter element groups than that of the former one. So it is assumed that the uniform cleaning for all filter elements subjected to ongoing cleaning by pulse-jet, and the pressure drop rise versus time is linear as shown in Eq. (4) and Eq. (5) to simplify the calculation

work of pressure drop using the rising rate of temporary pressure drop ( $r_C$ ).

$$\Delta P_C = r_C t \tag{4}$$

$$r_C = \frac{(\Delta P - \Delta P_{i+1})}{(t_{i+1} - t_i)} \tag{5}$$

The number of filter elements belonging to one group is  $N/n$  when the overall number of  $N$  filter elements is divided into  $n$  groups. Each group is subjected to the successive pulse-jet after its operation run during  $n$  times of individual pulse cycle in the pulse mode based on the time-based cleaning (TBC). The pulse cycle depends mainly on the number of pulsing groups. Furthermore, the duration of pulse cleaning (pulse duration) is usually within the range of 0.1 to 1.5 seconds to maintain a certain overpressure in the filter cavity during the injection of pulse gas. The filter elements in the ongoing pulse cleaning group are exposed to the back flow force while the others to the forward flow force.

To obtain the general equation to predict the pressure drop rise versus time, two extreme cases of one group or three groups using three filter elements as a whole are inspected. All of the three filter elements are congregated in one group to simulate the case of one group. All the three filter elements are also cleaned concurrently during a pulse-jet. Otherwise, each filter element is cleaned successively in a given pulse cycle to simulate the case of three groups of the filter unit. Considering that the pulse cycle is 3 min, the pulse-jet of cleaning gas is injected into the operating filter elements every 3 minutes successively for the case of three groups and every 9 min for the cases of one group as shown in Fig. 2.

Fig. 2(a) presents a schematic diagram denoting the change of cumulative particle load on the filter surface during the run time of the filtration (until the moment of the pulse gas injection). The painted-area in the bar means the particle load fraction covering the filter surface of each element during the duty of pulse cycle. The area

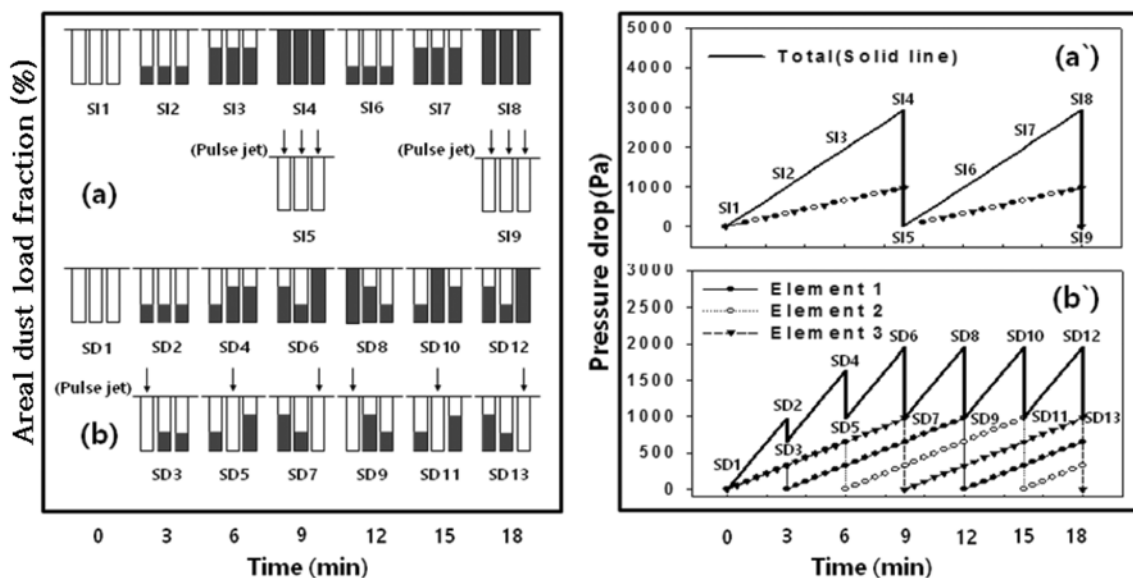


Fig. 2. Schematic expression denotes the fractional surface coverage of the dust load on the filter elements and corresponding pressure drop during the pulse-jet for two different grouping modes: (a) and (a') for one group; (b) and (b') for three groups.

indicates the relative quantity of dust load compared with that of the whole cycle, which corresponds to the dust loading time during the ongoing filtration until the next pulse cleaning time. In case of one group, all of the dust cakes attached on the filter element during the filtration run are dislodged at the same time on the pulse cleaning. The formation of the dust cake then starts from the base from which the surface of all elements is cleaned; it also begins from the lowest pressure drop as shown in Fig. 2(a). Pressure drop across the dust cake is linearly proportionate with the area mass load of the filter element [20,26], so pressure drop across the individual element belonging to the group is also proportionate linearly with the run time [26]. Total pressure drop of the filter unit represents the summation of that across the individual filter element. When the pulse cycle is set up with 9 min for one group case in order to compare the rising pattern of the pressure drop in the same condition with the case of three groups, the surface covering of dust cake continues during 9 minutes with the successive progress of 3 minutes (state 2; SI2), 6 minutes (SI3), finally reaching state 4 (SI4), and then all of the temporary dust cakes are dislodged from the surface of all the three filter elements to return to the original state (SI5 or SI1). The next pulse jet occurs at state 8 (SI8) after the next minutes again and returns to state 9 (SI9). Here, SI4 and SI8, as well as SI1, SI5, and SI9, cannot be distinguished. Thus, SI4 represents the state corresponding to the peak pressure drop of the filter unit. Further, SI1 represents the state corresponding to the lowest pressure drop of the filter unit and indicates the pressure drop when the filter elements are cleaned with the pulse-jet. Therefore, SI4 and SI1 are repeated to make the peak and the base line pressure drops, respectively.

When the filtration starts using the three fresh filter elements as shown in Fig. 2(b) for the case of three groups, areal mass load reaches State 2 (SD2) after 3 minutes during the first pulse cycle. The pulse cycle of 3 minutes is chosen to match with the case of one group with its value being 1/3 times. At the moment of first pulse injection, 1/3 dust load according to the total filter element surface is covered on each element, and the first filter element is subjected to be cleaned to leave SD3 after the first pulse cleaning. The pressure drop reduction with the first pulse cleaning corresponds to that across the first filter element. The next filtration continues to reach SD4 during the second pulse cycle of 3 min. At this time the surface coverages of each filter element are 1/3, 2/3, and 2/3, respectively, for the first, second, and third elements. The second pulse-cleaning makes state SD5. The pressure drop reduction with the second pulse cleaning corresponds to that across the second filter element and two times of the first one. The third step makes SD6 where 2/3, 1/3, and 3/3 of the filter surface are covered for the first, second, and third elements, respectively. Further pulse cleaning for third filter element makes SD7, which represents the state corresponding to the base line pressure drop in case of three groups. The pressure drop reduction with the third pulse cleaning corresponds to that across the third filter element and three times to the first one. After this step, SD6, SD8, and SD10 are successive, which are not distinguishable from each other, denoting the states corresponding to the peak pressure drop for the case of three groups. SD7, SD9, and SD11 denote the state for the base line pressure drop. These two states repeat for every pulse cleaning.

The dust coverage at maximum peak is 2/3 of the full dust load for total elements, and the dust coverage at the minimum state of base line pressure drop is 1/3 of the full one. Thus, the rising pattern of pressure drops in the case of three groups lies between the minimum and the maximum values as shown in Fig. 2(b) corresponding to the fractional surface coverage mentioned above. It is evident that the peak pressure drop becomes lower, with the number of pulse groups increasing as the fractional surface coverage decreases. Thus, the peak pressure drop gets lower as the number of filter element group increases.

A statistical approach is necessary to generalize the model. First, the surface coverage of dust cake during the filtration time, which is proportional to the pressure drop across the filter element, is considered. The total exposure fractions (corresponding to the summation of the dust load on the individual filter elements during the service time) to the dust load are the relative values compared with the whole pulse cycle of one group, and those are 1, (1+2)/4, (1+2+3)/9, and (1+2+3+4)/16 for the case of 1, 2, 3, and 4 pulse groups, respectively. The extension of this rule makes the general Eq. (6), denoting the total fraction of run time for the case of  $n$  groups. Further, this value is a fraction of the dust cakes remaining on the total filter elements just at the time when the pulse-jet works to clean one group among the total groups. Thus, the run time, or filtration time, for dust accumulation corresponding to the state presenting the peak pressure drop ( $\Delta P_{Cmax}$ ) is expressed as Eq. (7) by multiplying the pulse cycle, where  $\tau_i$  is the pulse cycle for the whole groups, which means the pulse cycles for individual group are  $\tau_i$ ,  $(1/2)\tau_i$ , and  $(1/3)\tau_i$  for the case of one, two, and three divisions of the pulse groups, respectively. It is expressed as  $(1/n)\tau_i$  in general. Therefore,  $\Delta P_{Cmax}$  and  $\Delta P_{Cmin}$  are expressed by Eq. (8) and Eq. (9), respectively, by multiplying the filtration time by the pressure drop rising rate ( $r_C$ ). Total pressure drop ( $\Delta P_T$ ) and base line pressure drop ( $\Delta P_B$ ) of the filter unit at a given run time  $t$  can be calculated by Eq. (10) and Eq. (11), respectively, where  $\Delta P_F$  is the pressure drop across the fresh filter element and is basically expressed with the Darcy's law on the effect of the filter element and operational condition. However, conditional analysis of pressure drop is beyond this paper. It is usually about 500 Pa for the fresh ceramic candle of Dia-Shumalith-10 (from Schumacher Co.) at the face velocity of 0.02 m/s. The values of  $r_R$  and  $r_C$  would be determined from the experiment in this study in order to apply the simple equation as possible as for the observation of the pressure drop trend according to the number of pulse groups.

$$\text{Total exposure fractions} = \frac{1}{n} \sum_{i=1}^n i \quad (6)$$

$$\text{Total run time} = \tau_i \frac{1}{n} \sum_{i=1}^n i \quad (7)$$

$$\Delta P_{Cmax} = r_C \tau_i \frac{1}{n} \sum_{i=1}^n i \quad (8)$$

$$\Delta P_{Cmin} = r_C \tau_i \frac{1}{n} \sum_{i=1}^{n-1} i \quad (9)$$

$$\Delta P_T = \Delta P_F + r_R t + r_C \tau_i \frac{1}{n} \sum_{i=1}^{n-1} i \quad (10)$$

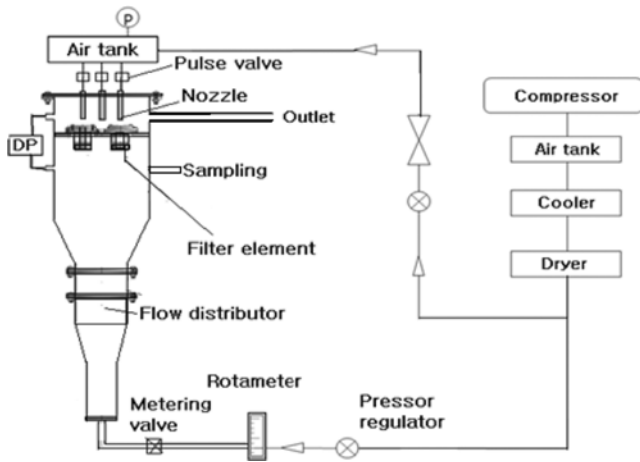


Fig. 3. Experimental unit for the measurement of pressure drop of filter unit using an entrainment bed: DP Differential pressure transmitter.

$$\Delta P_B = \Delta P_F + r_R t \quad (11)$$

## EXPERIMENTAL METHODS

A test facility was set up to measure the overall pressure drop of the filter unit inserted in an entrained-bed column as shown in Fig. 3. The experimental unit provides the uniform dust stream of constant face velocity and dust concentration by the principle of the entrainment fluidizing. The particles in a special size range corresponding to the superficial velocity of air in the bed are entrained in the air stream and approach the filter elements to be accumulated on their surfaces while the clean gas passes out. The dust cakes are detached from the filter surfaces during the pulse cleaning and are settled downward but dispersed again in the air stream supplied from the bottom of the entrained-bed to form the dust stream in the bed. The tube sheet, where the filter elements are mounted, divides the filter unit into the clean room and the dust chamber. Three filter elements of cylindrical type (in the length of 200 mm) are prepared by the cutting of an industrial filter element (DIA-Shumalith 10-20 from Shumacher Co.) and mounted

on the tube sheet. The physical properties of DIA-Shumalith 10-20 are described in reference [2]. The concentration and size distribution of the particles in the dust room are measured using the sample collected from the sampling tube, which is connected in the dust chamber.

The pulse-jet generating system consists of a pulse air tank, connecting pipe-work, fast-acting valve (pulse valve), and nozzle. The reservoir volume of the compressed air is 0.03 m<sup>3</sup> and maintains a given pressure for the pulse-jet. Straight nozzles with an inner diameter of 8 mm are fixed on the position of 30 mm above the filter mouth and connected to the pulse valves which are also connected to the pulse air tank. The differential pressure between clean room and dust chamber is measured with a differential pressure transmitter (ST3000 S900 from Honeywell Co.) and its variation versus time is recorded with a personal computer. Three normally closed solenoid valves, whose orifice size is 15 mm and flow coefficient is 0.02 m<sup>3</sup>/s-bar, are used. Total flow rate of the filter unit is measured using a flowmeter and controlled using a metering valve to meet the amount corresponding to the face velocity of 0.02 m/s in the filter element.

The filter elements are cleaned in two modes at the conditions shown in Table 1. Mode one is time based cleaning (TBC) method where pulse gas is injected at a given pulse cycle for every filter element in the group successively in order. The other is pressure based cleaning (PBC) method where pulse gas injection occurs when the pre-set peak pressure reaches a certain value. Pressure drop change versus time is recorded for the two cases. Three filter elements are cleaned at the same time for the simulation case of one group and one of three elements is cleaned successively at a given pulse cycle for the simulation case of three groups. To realize a similar operational condition with the case of three groups, the pulse cycle for one group is determined with the value of three times (9 minutes) of one group where the pulse cycle is 3 minutes. The pulse gas injection for the three filter elements is completed within 3 seconds of the successive injection with a short time interval of 1 s for each element to realize the concurrent pulse cleaning. The face velocity and pressure of the pulse air tank are fixed with the values of 0.02 m/s and 5 bars for all the experiments.

The particulate used in the study is the fly ash from a pilot unit

Table 1. Operation conditions of pulse-jet in the experimental unit

Filter element grouping mode	One group	Three group
Filter element		
- Length [mm]	200	200
- Surface area per group [m <sup>2</sup> ]	0.104	0.034
Particle concentration [g/m <sup>3</sup> ]	366	366
Mean particle size [μm]	3.45	3.45
Element number in a group	3 Elements	1 Element
Operation Temperature	Room temperature	Room temperature
Operation pressure	Atmospheric pressure	Atmospheric pressure
Face velocity [m/s]	0.02	0.02
Pulse air pressure [bar]	5	5
Pulse cycle [min]	9	3
Pulse duration [s]	0.3	0.3

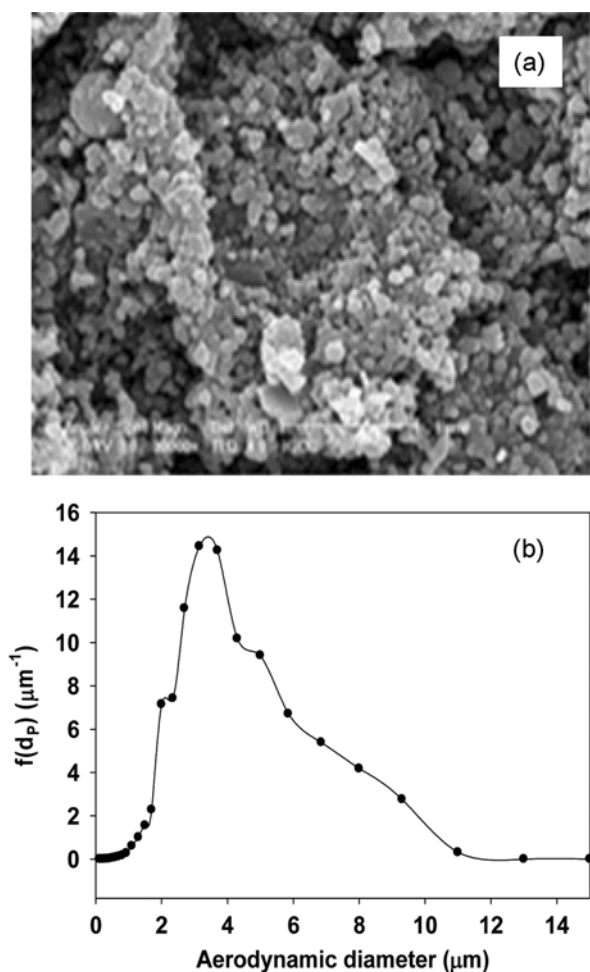


Fig. 4. SEM image (a) and the particle size distribution (b) measured with API of the entrained fly ash from the experimental unit.

of integrated coal gasification (ICG) carried out at the Institute for Advanced Engineering (IAE) in Korea. Proper amount of fly ash is filled in the bed initially and entrained in the applied air of a constant flow rate to meet the required face velocity in the filter element, supposing that it is all consumed for the filtration gas. The particle concentration in the bed is measured with the mass change of an absolute filter at the experimental operation condition and is controlled in the value of  $366 \text{ g/m}^3$  by the adjustment of ash amount and flow rate. The entrained particulates in the experimental condition for the filtration face velocity  $0.02 \text{ m/s}$  are composed of nearly spherical particles as shown in Fig. 4(a) observed with a secondary electron microscope. The particle size distribution of this sample, which is sampled in the bed during the normal operation run as shown in Fig. 4(b), is measured with an aerodynamic particle size analyzer (A AEROSIZER LD). The geometric mean diameter of this sample is  $3.45 \text{ μm}$ .

## RESULTS AND DISCUSSION

To determine the rising rate of the residual pressure drop ( $r_r$ ), the change of the base line pressure drop ( $\Delta P_B$ ) was measured for

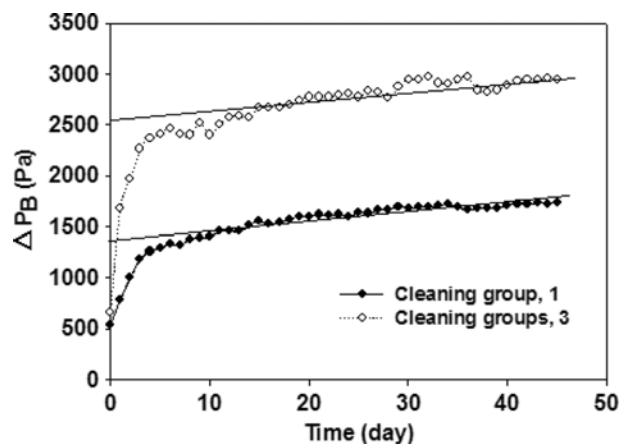


Fig. 5. Base line pressure drops versus time during the long run of the experimental filter unit.

over 45 days as shown in Fig. 5. The experimental results were obtained under two different modes of one group (dark circles) and three groups (open circles) with a pulse duration of  $0.3 \text{ s}$  at a pulse pressure of  $5 \text{ bar}$ .  $\Delta P_B$  in Fig. 5 denotes the pressure difference between the dust room and the clean room measured at the minimum pressure point right after the pulse air injection. It increases steeply at the initial conditioning stage of the filtration time when the fresh filter element is used from the initial start. The initial sharp increase of residual pressure drop stems from the formation of residual dust cake on the clean filter surface. This is called the conditioning stage where the residual dust cake is formed while parts of particles penetrate into the large pores of the filter element to inhibit the gas flow through it. The main resistance of flow comes from the dust cake which keeps the strong bonding force between the particles and/or the surface of the filter element in this stage. The value of  $\Delta P_B$  depends on several factors originating from the particle properties and operational conditions. The inspection of this variation is beyond the scope of this study; thus, the experimental measurement was adopted to develop a simple model using the simple Eq. for the rising rate of the residual pressure drop ( $r_r$ ).

The rising patterns of the base line pressure drop keep the increasing stable after 20 days for two cases and construct an approximately linear increase versus time. The rising rates of the residual pressure drop ( $r_r$ ) can be determined by the slope of this linear line. The rising rates of the residual pressure drop ( $r_r$ ) is  $4.25 \times 10^{-3} \text{ Pa/min}$  and is determined as the empirical value for usage in Eq. (10) and Eq. (11). The value at the starting point where the ordinate axis meets zero point of time in the linear line is chosen as the hypothetical base line pressure drop ( $\Delta P_{B,0}$ ) at time zero of the operation run. The values are  $1,380$  and  $2,500 \text{ Pa}$  for one group and three groups, respectively. The results in Fig. 5 show that the  $\Delta P_B$  of one group mode is lower than that of three groups mode, which means that the cleaning strength is stronger in case of one group mode. The reason for this result is all the temporary dust cakes on the filter surfaces are removed together in the case of one group, while the dust cakes on one of three elements are removed in case of three groups.

To obtain the empirical value ( $r_c$ ), the total pressure drop ( $\Delta P_T$ )

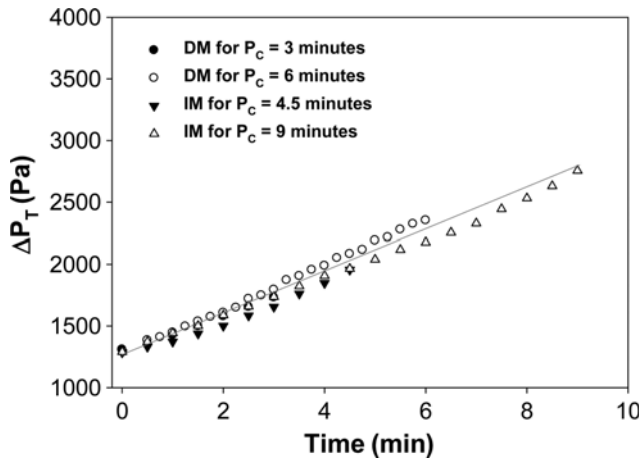


Fig. 6. Total pressure drop versus time measured at various pulse cycle conditions.

of the filter unit versus time was measured at several conditions of pulse cycles: 3 min (●) and 6 min (○) for the case of three groups, as well as 4.5 min (△) and 9 min (▼) for one group mode at the same condition for the measurement of  $r_r$  mentioned above. Careful inspection of the curves versus time shows a slightly concave shape with the time increase. However, this also satisfies the linear regression for a general linear curve versus time with the regression coefficient of more than 99%. Thus, the increasing rate of pressure drop across the temporary dust cake ( $r_c$ ) is calculated with the slope of the general linear curve (straight line) and is 148 Pa/min for the empirical value of this study.

### 1. Pressure Drop of the Filter Unit at Mode of Time Based Cleaning (TBC)

To verify the semi-empirical model for the prediction of the operation pressure drop of the filter unit, the calculated results are compared with experimental ones in Fig. 7 and Fig. 8 for the cases of one group and three groups, respectively. In one group mode, all of the three filter elements are cleaned concurrently every 9 minutes by the method of the consecutive pulse gas injection with a significantly short pulse cycle of 1 s for each filter element of three, which simulates the concurrent pulse cleaning of all the three filter ele-

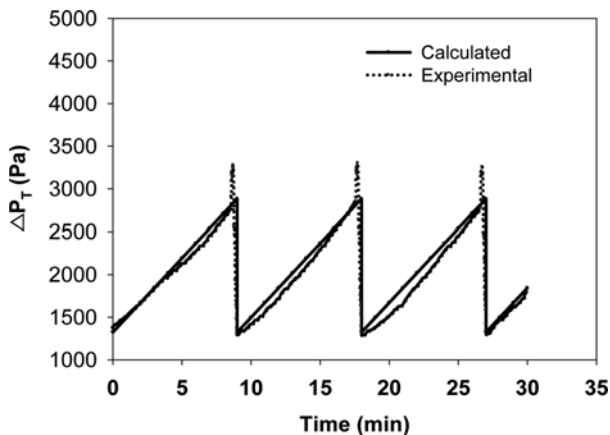


Fig. 7. Pressure drops calculated by Eq. (10) for one group to compare with the experimental values.

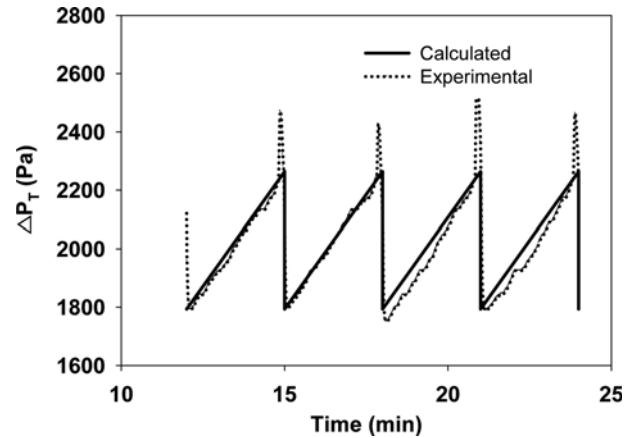


Fig. 8. Pressure drops calculated by equation 10 for three groups to compare with the experimental values.

ments overcoming the experimental restriction. The filter element is cleaned one by one successively every 3 min in three groups. The results in the figures show the total pressure drop versus time for those two cases in the normal operation condition with the pulse gas pressure of 5 bars and the pulse duration of 0.3 s. Total pressure drops calculated with Eq. (10) (solid lines) meet the values measured in the experimental unit (dash lines) well for two cases of one group (Fig. 7) and three groups (Fig. 8), respectively. The experimental results shown in Fig. 7 and Fig. 8 are compared in Fig. 9. The peak and the base line pressure drops are kept constantly at the values of 1,470 and 2,840 Pa/s for one group and 1,760 and 2,250 Pa/s for the case of three groups, respectively. These results indicate that one group mode presents a lower base line pressure and higher peak pressure than the case of three groups. This result comes from the same reason mentioned for Fig. 5 that more amounts of the temporary dust cakes on the filter surfaces are removed together in the case of one group, while a small amount of dust cakes on one of three elements are removed in the case of three groups.

Fig. 10 shows the change of the peak and the base line pressure drop according to the number of pulse groups which are calculated by Eq. (10) for the extension of pulse groups. The peak pres-

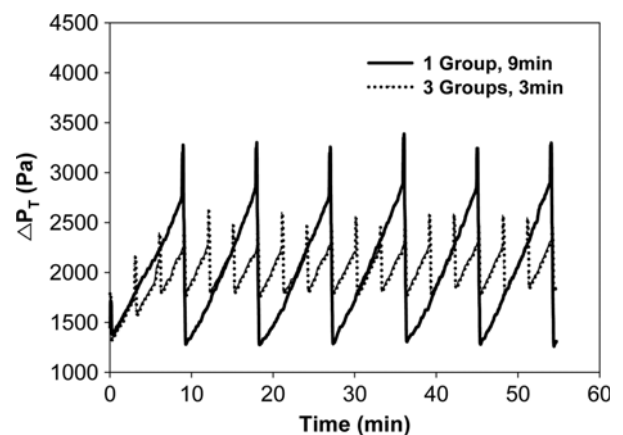


Fig. 9. Influence of pulse grouping on pressure drop changes of the filter unit.

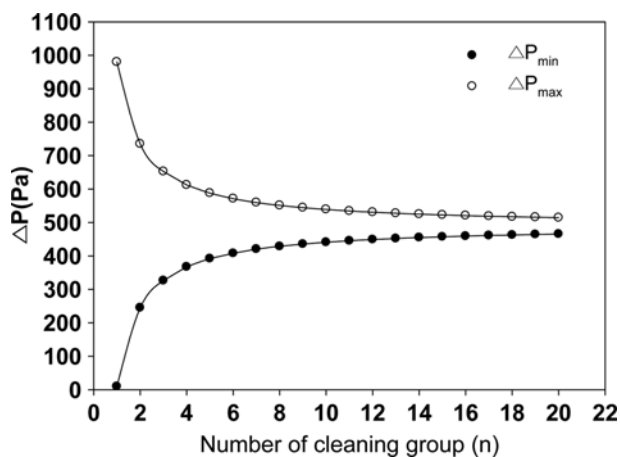


Fig. 10. Pressure drop changes of the maximum and the base line as the increase of the pulse group number.

sure drop ( $\Delta P_{max}$ ) decreases gradually and approaches a minimum equilibrium value as the number of the cleaning group increases. Otherwise, the base line (minimum) pressure drop ( $\Delta P_{min}$ ) increases and approaches a maximum equilibrium value gradually as the number of the cleaning group increases. Thus, the gaps between the peak and the minimum pressure drop become narrow as the number of filter grouping increases. This phenomenon of gap reduction is promising for the pulse cleaning of the filter element as it reduces the pulse cleaning load. The high value of the peak pressure drop requires a strong pulse force which requires a high pressure of pulse gas or/and long pulse duration (or the short pulse cycle). It is important to prepare the pulse conditions requiring weak cleaning force but providing effective cleaning of the filter element as much as possible to reduce the bad effects along the pulse cleaning such as malfunctions in the gas flow of the filter unit. The injection of high pressure pulse gas will provide a strong cleaning effect but also induce an intensive non-distribution on the gas flow in the filter unit, resulting to an unnecessary increase in filtering resistance, as well as high consumption of pulse gas.

Pressure drops of the base line and the peak value naturally increase as the pulse cycle increases as shown in Fig. 11, which shows

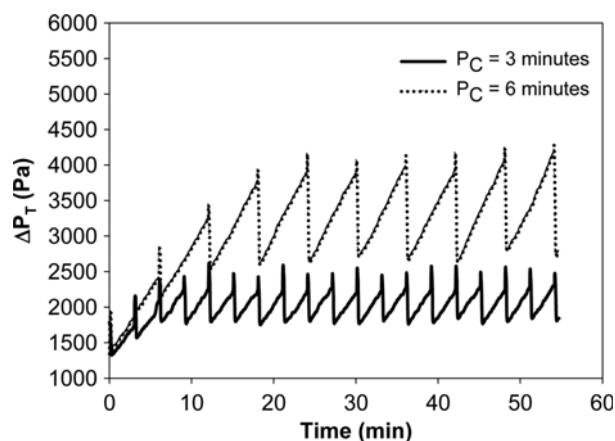


Fig. 11. Influence of the pulse cycle on pressure drop of the filter unit for three groups.

those values in case of pulse cycles for 3 and 6 minutes, respectively. The peak values of pressure drops are 2,280 and 3,950 Pa and the base line pressure drops are 1,800 and 2,750 Pa for the pulse cycles of 3 and 6 minutes, respectively. Naturally, the base line pressure drop should change along with the operational conditions. However, the change patterns of the base line pressure drop according to the number of pulse group are similar for all cases.

## 2. The Effect of the Pulse Cleaning Efficiency According to the Filter Group Number

Cleaning efficiency ( $\varepsilon$ ) of the filter element during pulse cleaning is defined as Eq. (12) by using the notations mentioned in Fig. 1. Perfect cleaning means the pressure drop ( $\Delta P$ ) should recover the starting value of the point  $\Delta P_i$  which is the value at the start time for a given cleaning cycle of time  $t_i$  as shown in Fig. 1(b). The cleaning efficiencies were almost 100% for all experiment cases in this study. However, the differences in cleaning efficiency during the short time operation are too small to judge for their effect on the pulse cleaning. Otherwise, the difference of the change is distinguishable even during several cycles for the case of the pressure based cleaning (PBC) method where the pulse cleaning is carried out when the pre-set peak pressure drop is reached; that is, the pulse condition providing the longer pulse cycle is more effective than the case of a shorter one. A longer pulse cycle for the same set pressure drop means a higher cleaning efficiency.

$$\varepsilon = \frac{\Delta P - \Delta P_{i+1}}{\Delta P - \Delta P_i} \times 100 \quad (12)$$

The cleaning efficiency according to the operation modes can be evaluated by comparing the pulse cycles with each other. Figs. 12 and 13 show the rising patterns of total pressure drop for one group and three groups, respectively, for the pre-set pressures of 1,960, 3,430, and 4,410 Pa. Pulse cycles for each case are summarized in Table 2. Every three cycles (corresponding to one cycle for one group) is considered as one cycle for three groups in the figures, because the starting point of three groups returns after each three cycles of individual filter element. The pulse cycle of three groups is longer than one group for all the cases, meaning the pulse cleaning effect for the case of three groups is more effective than that of one group.

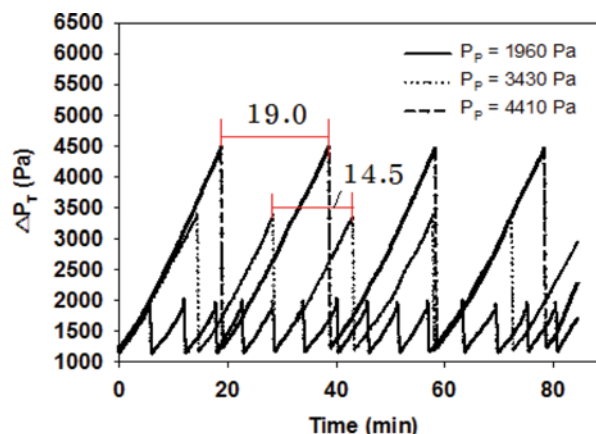


Fig. 12. Influence of the pre-set pressure on the pulse cycle variation for one group.

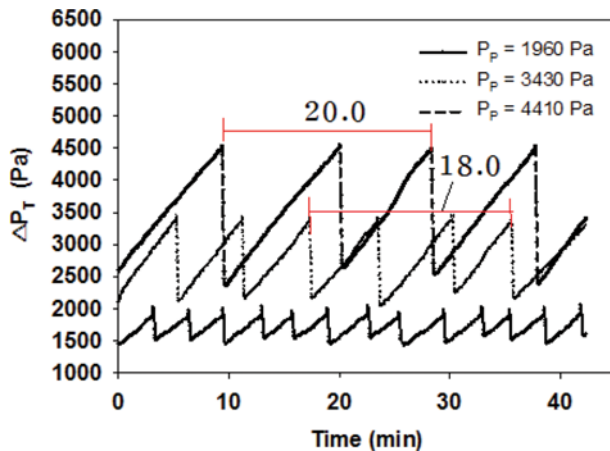


Fig. 13. Influence of the pre-set pressure on the pulse cycle variation for three groups.

Table 2. The pulse cycles [min] of filter unit to clean the filter element in the PBC operation modes

Pulse mode	One group	Three group
Pre-set pressure of 1,960 Pa	5.7	9.5
Pre-set pressure of 3,430 Pa	14.5	18.0
Pre-set pressure of 4,410 Pa	19.0	20.0

## CONCLUSIONS

A semi-empirical model was developed to predict the pressure drop of a ceramic filter unit and to see the effect of the grouping number of filter elements. The model applies a statistical approach, as well as the Darcian-type equation, but uses the simple experimental equation for the pressure drops across the residual and the temporary dust cakes which have the linear dependency versus filtration time, respectively. It is also assumed that the pressure drop is proportional to the fractional surface coverage (over that for the full time service) of the dust load corresponding to the pulse cycle. The model is verified with the experimental values for two cases of simulation groups of filter elements (one and three groups using three filter elements) in an entrainment-bed column.

The experimental observation of pressure drop rise meets well with the model-calculation values. From the basis of this result a general equation is obtained to predict the pressure drop rise versus the filtration time. The theoretical equation predicts the operation values of the pressure drop between the peak and the base line, which suggests the practical guideline for grouping the filter elements in the preliminary design of the filter unit. The peak pressure drop decreases and approaches a minimum equilibrium value as the number of the cleaning group increases. Otherwise, the base line pressure drop increases and approaches a maximum equilibrium value as the number of the cleaning group increases. The gaps between the peak and the base line pressure drop become smaller as the number of filter group increases. This phenomenon of the gap reduction between the peak and base line pressure drop is promising as it reduces the pulse cleaning load. The pulse cleaning becomes more effective as the number of the cleaning groups

increases from the observation of the pulse cycle variation in the pressure-based operation mode.

## ACKNOWLEDGEMENTS

This work was supported by the Korea Institute of Energy Technology Evaluation and Planning (KETEP) grant funded by the Korean government's Ministry of Knowledge Economy (No. 2011201020004C).

## REFERENCES

1. J. P. K. Seville, S. Ivatt and G. K. Burnard, *High Temperature Gas Cleaning*, Ed. by E. Schmidt et al., University of Karlsruhe, 23 (1996).
2. S. Heidenreich, *Fuel*, **104**, 83 (2013).
3. B. Dou, C. Wang, H. Chen, Y. Song, B. Xie, Y. Xu and C. Tan, *Chem. Eng. Res. Design*, **90**, 1901 (2012).
4. K. Schulz and M. Durst, *Filtration and Separation*, **31**(1), 25 (1994).
5. H. Chi, L. Yu, J. H. Choi and Z. Ji, *Chinese J. Chem. Eng.*, **16**(2), 306 (2008).
6. Z. Ji, M. Shi and D. Fuxin, *Powder Technol.*, **139**, 200 (2004).
7. I. Schildermans, J. Baeyens and K. Smolders, *Filtration and Separation*, **41**(5), 26 (2004).
8. A. R. Mazaheri and G. Ahmadi, *Adv. Powder Technol.*, **17**(6), 623 (2006).
9. Z. Ji, S. Peng and L. Tan, *Chinese J. Chem. Eng.*, **11**(6), 626 (2003).
10. G. Ahmadi and D. H. Smith, *Aerosol Sci. Technol.*, **36**, 665 (2002).
11. J. H. Choi, Y. G. Seo and J. H. Chung, *Powder Technol.*, **114**, 129 (2001).
12. S. K. Grannell and J. P. K. Seville, *Proceedings of the 4<sup>th</sup> International Symposium on Gas Cleaning at High Temperatures*, A. Dittler, et al. Ed., Karlsruhe, Germany, 96 (1999).
13. D. H. Smith, V. Powell and G. E. I. Ahmadi, *Powder Technol.*, **94**, 15 (1997).
14. X. Simon, S. Chazelet, D. Thomas, D. Berner and R. Regnier, *Powder Technol.*, **172**, 67 (2007).
15. J. H. Choi and G. w. Park, *Energy Eng. J.*, **8**(1), 143 (1999).
16. J. H. Choi, S. J. Ha and Y. O. Park, *Korean J. Chem. Eng.*, **19**(4), 711 (2002).
17. J. H. Choi, S. J. Ha, Y. C. Bak and Y. O. Park, *Korean J. Chem. Eng.*, **19**(6), 1085 (2002).
18. J. H. Choi, Y. C. Bak, H. J. Jang, J. H. Kim and J. H. Kim, *Korean J. Chem. Eng.*, **21**(3), 726 (2004).
19. Y. Endo, D.-R. Chen and D. Y. H. Pui, *Powder Technol.*, **98**, 241 (1998).
20. J. H. Choi, S. J. Ha and H. J. Jang, *Powder Technol.*, **140**, 106 (2004).
21. A. Gupta, V. J. Novick, P. Bisawas and P. R. Monson, *Aerosol Sci. Technol.*, **19**, 94 (1993).
22. R. Dennis and J. A. Dirgo, *Filtration and Separation*, **18**, 394 (1981).
23. C. R. N. Silva, V. S. Negrini, J. R. Aguiar and M. L. Coury, *Powder Technol.*, **101**, 165 (1999).
24. J. H. Kim, Y. Liang, K. M. Sakong, J. H. Choi and Y. C. Bak, *Powder Technol.*, **181**, 67 (2008).
25. M. L. Aguiar and J. R. Coury, *Ind. Eng. Chem. Res.*, **35**, 3673 (1996).
26. M. lupion, B. Alonso-Farinas, M. Rodriguez-Galan and B. Navarrete, *Chem. Eng. Processing*, **66**, 12 (2013).